



# Production of *n*-butyl levulinate over modified KIT-6 catalysts: comparison of the activity of KIT-SO<sub>3</sub>H and Al-KIT-6 catalysts

Alireza Najafi Chermahini<sup>1</sup> · Matin Assar<sup>1</sup>

Received: 20 October 2018 / Accepted: 15 April 2019  
© Iranian Chemical Society 2019

## Abstract

The catalytic activity of propylsulfonic acid-functionalized mesoporous silica (KIT-SO<sub>3</sub>H) was compared to the performance of alumina-incorporated KIT-6 (Al-KIT-6) in the esterification reaction of the biomass-derived levulinic acid with *n*-butanol. The catalysts were prepared by functionalization of the silica support with propylsulfonic acid (Pr-SO<sub>3</sub>H) by post-synthesis grafting using 3-mercaptopropyltrimethoxysilane as a propyl-thiol precursor followed by oxidation. In addition, Al-KIT-6 was synthesized according to in situ synthesis. Catalysts were characterized using various techniques such as XRD, nitrogen adsorption/desorption, SEM, TGA, ICP-OES, FT-IR and elemental analysis. It is evident that increases in catalyst loading, butyl alcohol-to-levulinic acid ratio and reaction temperature significantly enhance the butyl levulinate yield. The reusability and stability of catalysts were evaluated, and it was found that while esterification reaction by KIT-SO<sub>3</sub>H compound catalyzed under milder conditions, the stability of Al-KIT-6 catalyst was better.

**Keywords** Esterification reaction · Butyl levulinate · Levulinic acid · Solid acid catalyst · KIT-6

## Introduction

Confident technology for its progress needs initial sources of energy and material. Therefore, replacement of fossil fuel-based technologies with renewable and sustainable technologies which consume biomass-derived materials is necessary. One of the top 10 important compounds derived from biomass is levulinic acid (LA) [1–3] that has been utilized as a precursor for the production of chemicals, such as *gamma*-valerolactone (a green solvent and potentially useful polyester monomer) [4, 5], methyltetrahydrofuran [6] (a valuable solvent or gasoline blending component), methyl vinyl ketone [7] and  $\alpha$ -angelica lactone [8]. Among the LA derivatives, alkyl levulinates such as methyl, ethyl, propyl and butyl levulinates are of particular interest due to their specific physicochemical properties such as flash point

stability, high lubricity and moderate flow properties under the low temperature that make their properties similar to traditional fuel additives [9–11]. In addition, like other esters with a short-chain alkyl group, the alkyl levulinates find extensive application either in the flavoring and fragrance industries [12, 13]. For example, *n*-butyl levulinate has been used in organic process industries for different purposes such as plasticizing agent, solvents and odorous substances [14–16]. Generally, alkyl esters of levulinic acid can be prepared by the esterification of LA with alcohols or alcoholysis of furfuryl alcohol [17–20]. Various homogeneous [21–23] or heterogeneous catalysts [24–26] have been utilized in the esterification of LA with alcohols. With more attention to the progress of green processes, many efforts have been made to advance environmentally friendly technologies for esterification reactions. So, various heterogeneous catalysts have been reported for conversion of LA to alkyl levulinates. For example, Tejero et al. [27] have reported esterification of LA with 1-butanol over ion exchange resins. They have found that butyl levulinate (BL) yields were in the range of 90.5–93.5% with 99.5% selectivity. Recently, Zhou et al. [28] have used a modified phosphotungstic acid as a novel efficient catalyst for the synthesis of *n*-butyl levulinate. They found 99% yield but did not report any catalyst recycling. Cirujano et al. [29] used zirconium-containing MOF to

**Electronic supplementary material** The online version of this article (<https://doi.org/10.1007/s13738-019-01677-4>) contains supplementary material, which is available to authorized users.

✉ Alireza Najafi Chermahini  
anajafi@cc.iut.ac.ir; najafy@gmail.com

<sup>1</sup> Department of Chemistry, Isfahan University of Technology, 84154-83111 Isfahan, Iran

synthesize *n*-butyl levulinate and observed that the product formed quantitatively after 5 h.

In the present paper, a mesoporous silica material KIT-6 was synthesized and characterized. The KIT-6 material was then functionalized with aluminum through in situ synthesis or grafted by propylsulfonic acid groups and used as the solid acid catalyst to the conversion of biomass-derived levulinic acid to *n*-butyl, levulinate. For this purpose, reaction conditions such as temperature, amount of the catalyst loading, and the effect of reaction time were optimized. In addition, the recycling and reusability of the catalysts under optimized reaction conditions are achieved.

## Experimental

### Materials and instruments

Tri-block copolymer (Pluronic P123), levulinic acid, *n*-butanol, tetraethyl orthosilicate (TEOS, 98%), aluminum *iso*-propoxide (98%), 3-mercaptopropyltrimethoxysilane, and all of the used solvents were purchased from Sigma–Aldrich. All of the other chemicals were analytical grade and were applied without further purification. The nitrogen adsorption/desorption isotherms were collected at 77 K by using a PHS-1020 (PHSCHINA) device. The morphology of the catalysts was evaluated by SEM analysis on a VEGA\\TESCAN-LMU microscope, and high-resolution transmission electron microscopy (HRTEM) was used with a Philips CN120 device. Powder X-ray diffraction (XRD) patterns of samples were taken using a Asenware XDM-300 diffractometer using Ni-filtered Cu K $\alpha$  ( $K=0.15406$  nm) radiation. Elemental analysis was carried out by a CHNS analyzer (Elementar, Vario EL III).

### Catalyst preparation

#### Synthesis of KIT-6

The synthesis of mesoporous KIT-6 material was achieved by dissolving P123 as a structure directing agent and *n*-butanol as a co-solvent under acidic conditions. The preparation of the mesoporous silica was carried out as follows: 7.0 g of Pluronic P123 was dissolved in 253 g of distilled water and 13.7 g of HCl solution (35 wt%). Then *n*-butanol (4.0 g) was added at once to the above mixture, under vigorous stirring at 35 °C. Then, TEOS (15.05 g) was added and the solution was stirred for 24 h. After that, the suspension was kept under static conditions at the same temperature. Then, the solid product obtained was filtered without any washing and dried at 100 °C for 12 h. Finally, the template was removed by calcination of prepared silica at 550 °C for 6 h.

#### Synthesis of Al-KIT-6 and KIT-SO<sub>3</sub>H catalysts

Functionalization of KIT-6 with sulfonic acid groups was achieved by a previously reported method [30]. Briefly, to a mixture of 30 mL of dry toluene and 2 mL of 3-mercaptopropyltrimethoxysilane (MPTMS), 1.00 g of mesoporous KIT-6 was added and the mixture was refluxed for 24 h. The thiol-functionalized precipitate was filtered and then soxhleted with methanol as the extractor solvent, and then, the catalyst was dried at 80 °C overnight. In the next step, the mercapto groups were oxidized into –SO<sub>3</sub>H groups using hydrogen peroxide as the oxidant under stirring for 24 h at room temperature. The final product was filtered and washed with methanol and oven-dried at 80 °C overnight. The preparation of aluminum-modified KIT-6 was done according to the previous report with some modifications [31]. Shortly, 2.4 g Pluronic P123 was dissolved in 86.4 g water followed by the addition of 4.7 g HCl (35%) at 35 °C. To this mixture was added 2.4 g *n*-butanol and was stirred for 1 h, followed by the addition of 2.6 g TEOS and 0.4 g aluminum *iso*-propoxide as the aluminum source. The mixture was aged at 100 °C under static condition for 24 h. Finally, the white precipitate was filtered, dried at 100 °C and calcined at 550 °C to remove organic template.

#### Esterification of levulinic acid

Esterification of LA with *n*-butanol was performed under atmospheric pressure. In a typical catalytic reaction, 5 mL *n*-butanol and 0.615 g LA were added to a round-bottomed two-necked flask and was heated in the presence of 50 mg of mesoporous KIT-6-Al or KIT-SO<sub>3</sub>H under continuous stirring. Then, the reaction mixture was cooled and centrifuged, and the solid catalyst was recovered for recycling and reusing in the next run. For this purpose, the KIT-SO<sub>3</sub>H catalyst was thoroughly washed with acetone and dried at 120 °C and reused. For the recycling of KIT-6-Al catalyst, the solid was washed with acetone, and dried and calcined at 120 °C and 500 °C for 3 h, respectively. It is notable that to examine the reproducibility of the results, the esterification of LA with alcohols were performed in duplicate.

#### Reaction monitoring and product identification

The progress of the reaction was monitored on an Agilent (6890 N) gas chromatograph equipped with a flame ionization detector and using a DB5 capillary column (30 m  $\times$  0.25 mm, DF = 0.25  $\mu$ m), using helium as the carrier gas and air for the detector function (total flow of 1.3 mL/min). For the determination of butyl levulinate in the

samples, calibration curve by analyzing standard solutions with known amounts of products was used.

Butyl levulinate yield was calculated according to the following equation:

$$\text{Yield (mol\%)} = \frac{\text{moles of produced alkyl levulinate}}{\text{moles of starting LA}} \times 100 \quad (1)$$

For identification of products, GC-MS analysis was performed and the results are presented in the supplementary information.

## Results and discussion

### Catalyst characterization

Low-angle XRD measurements were used to study of ordering degree of samples. For the KIT-6 sample, Bragg reflections appeared at  $2\theta = 0.98, 1.2$  and  $1.69$ , degree corresponding to (2 1 1), (2 2 0) and (4 2 0) reflections, respectively (Fig. 1).

The results confirm the formation of well-ordered mesoporous material with  $1a3d$  bicontinuous cubic space [32]. For the KIT-SO<sub>3</sub>H and Al-KIT-6 catalysts, the intensity of sharp peak at the  $2\theta = 0.98$  was decreased probably because of the introduction of Al<sub>2</sub>O<sub>3</sub> or propylsulfonic acid groups. However, the position of the diffraction peak is not obviously changed, indicating the order of structure is intact.

It is known that the surface area and pore size of heterogeneous catalysts are of the highest importance because of their role in the diffusion of the reagents to the active sites. Figure 2 shows the adsorption-desorption isotherms of KIT-6, KIT-6-Al and KIT-Pr-SO<sub>3</sub>H samples, exhibiting type IV isotherms with H1 hysteresis loop according to the IUPAC classification. The samples show sharp nitrogen capillary condensation step in the  $P/P_0$  between 0.5 and 0.9 which

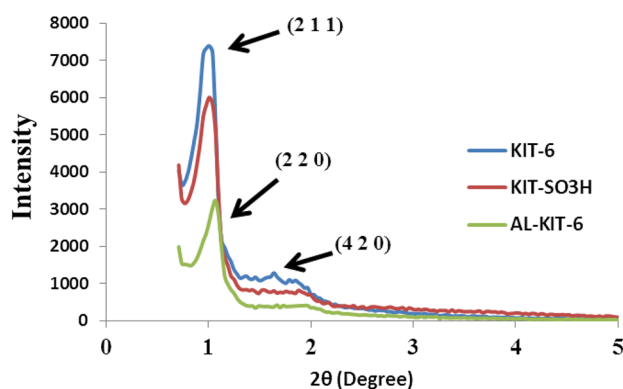


**Fig. 1** Small-angle XRD patterns of KIT-6, KIT-SO<sub>3</sub>H and Al-KIT-6 samples

is the characteristic of large and uniform mesopores with narrow pore size distribution. In addition, the corresponding pore size distribution curves estimated from the BJH method are plotted in Fig. 2. The formation of large and uniform channel-like ordered mesopores is evident by the narrow pore size distribution within a range of 2–7 nm.

The textural properties of the samples are presented in Table 1. For the pristine KIT-6, BET surface areas, pore size and pore volume were  $840 \text{ m}^2 \text{ g}^{-1}$ ,  $3.15 \text{ nm}$  and  $0.797 \text{ cm}^3 \text{ g}^{-1}$ , respectively. After surface modification with propyl-sulfonic acid groups, the  $S_{\text{BET}}$  and pore volume changed to  $394 \text{ m}^2 \text{ g}^{-1}$  and  $0.592 \text{ cm}^3 \text{ g}^{-1}$ , respectively. In addition, after alumina loading, the BET surface area and pore volume drastically reduced to  $175 \text{ m}^2 \text{ g}^{-1}$  and  $0.287 \text{ cm}^3 \text{ g}^{-1}$ , respectively. This indicates that some pores were blocked during surface modification. Pore size distribution was intact after surface modification of KIT-6.

The surface morphology of pristine KIT-6, KIT-Pr-SO<sub>3</sub>H and KIT-6-Al catalysts were analyzed by SEM technique (Fig. 3). The SEM image of KIT-6 (Fig. 3a) displays large three-dimensional rock structure, a unique characteristic of the KIT-6. SEM image of KIT-6-Al is compared with the morphology of KIT-6 which indicates that the surface morphology smoothness was not affected (Fig. 3b). Additionally, for the KIT-SO<sub>3</sub>H catalyst, the SEM image shows the irregular shape and the morphology was rough (Fig. 3c). The TEM image of KIT-6 mesoporous material is displayed in Fig. 3d, showing a three-dimensional cubic arrangement of pores with  $1a3d$  space group.

For the evaluation of the total organic content of KIT-SO<sub>3</sub>H sample, the thermogravimetric analysis results of pristine KIT-6 and KIT-SO<sub>3</sub>H catalyst with heating from room temperature to  $800 \text{ }^\circ\text{C}$  under N<sub>2</sub> atmosphere are provided in Fig. 4. For the KIT-6, total reduction of 3% in the weight occurred below  $150 \text{ }^\circ\text{C}$  related to losing moisture. With keeping in mind about 3% adsorbed water, the total organic content of 11% assigned to the KIT-SO<sub>3</sub>H catalyst. This value corresponds to  $7 \text{ mmol g}^{-1}$  sulfonic acid groups anchored to mesoporous material. Furthermore, based on elemental analysis of KIT-SO<sub>3</sub>H catalyst, 1.64% sulfur which corresponds to  $5.1 \text{ mmol g}^{-1}$  sulfonic acid groups was anchored to the surface of KIT-6 mesoporous material. In addition, according to ICP analysis total aluminum loading on the surface of KIT-6-Al solid acid catalyst was determined 1.1%.

The FT-IR spectra of KIT-6, KIT-6-SO<sub>3</sub>H and Al-KCC-6 catalysts are presented in Fig. 5. For the samples the broad peak appeared at  $3650 \text{ cm}^{-1}$  is assigned to stretching vibration of hydroxyl groups. Moreover, the low-intensity peak at  $1630 \text{ cm}^{-1}$  is attributed to the water molecules adsorbed on the surface of KIT-6. The broad absorption bands around  $1100 \text{ cm}^{-1}$  are assigned to Si–O–Si unsymmetrical stretching vibration.

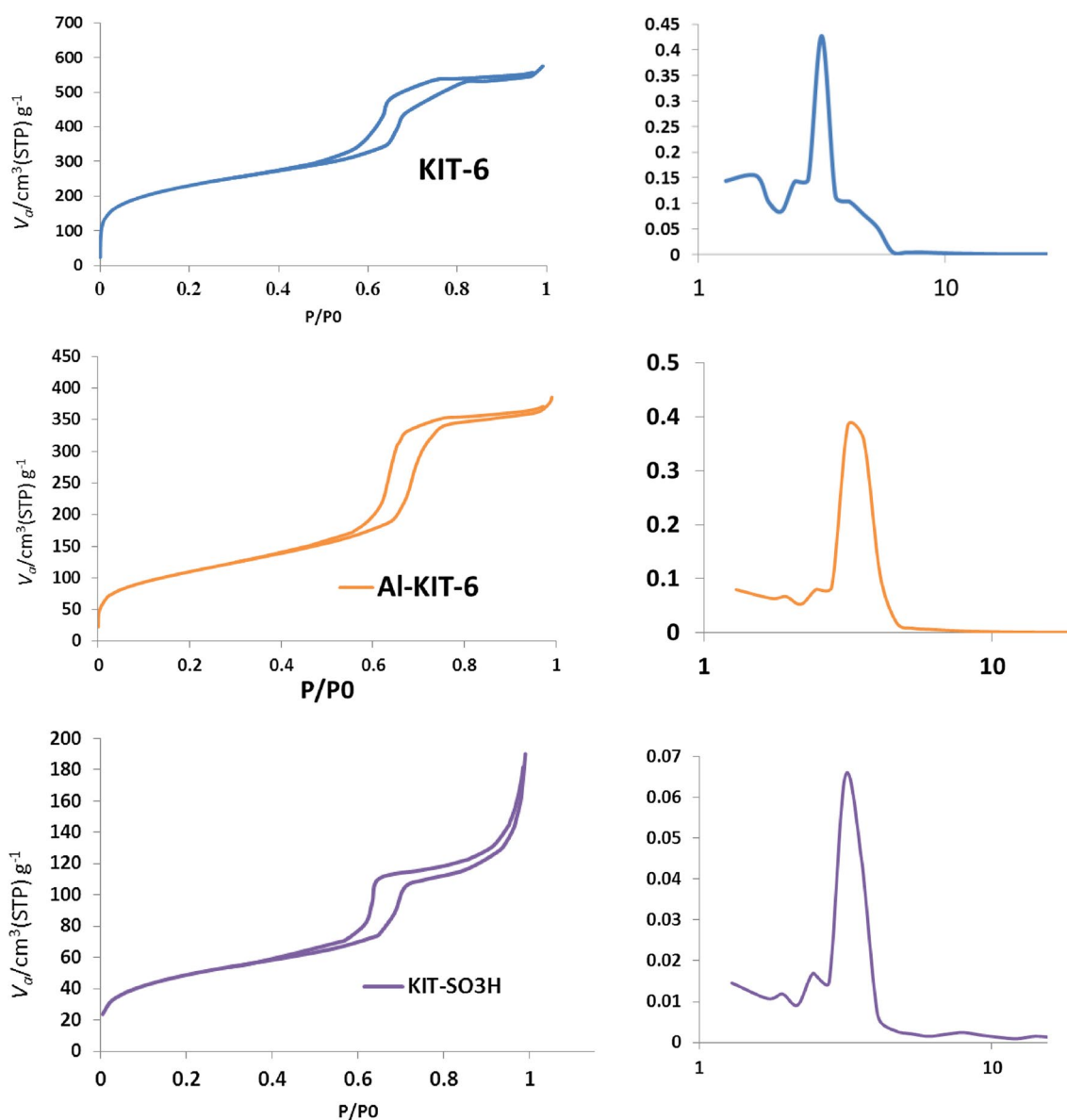


**Fig. 2** Nitrogen adsorption–desorption isotherms at 77 K of mesoporous KIT-6, KIT-SO<sub>3</sub>H and Al-KIT-6. The right column is the pore size distribution of samples

**Table 1** Textural properties of KIT-6, KIT-SO<sub>3</sub>H and Al-KIT-6

Sample	$S_{\text{BET}}$ (m <sup>2</sup> g <sup>-1</sup> )	$r_p$ (nm)	$V_T$ (cm <sup>3</sup> g <sup>-1</sup> )
KIT-6	840	3.15	0.797
KIT-SO <sub>3</sub> H	394	3.15	0.592
Al-KIT-6	175	3.15	0.287

$S_{\text{BET}}$  is the BET surface area deduced from the isotherm analysis

$r_p$  is the pore diameter calculated using the BJH method

$V_T$  is the pore volume at a relative pressure of 0.95

### Catalytic performance of the catalysts

In the present study, catalytic activity of a Bronsted solid acid catalyst (KIT-SO<sub>3</sub>H) is compared to a Lewis acid catalyst (Al-KIT-6) for the synthesis of butyl levulinate (BL). At first, KIT-SO<sub>3</sub>H was applied in the synthesis of BL from esterification of levulinic acid with *n*-butanol under the conditions of levulinic acid-to-butanol molar ratio of 1:6, 10 mg catalyst, in the temperature range of 70–120 °C and reaction time of 6 h. The experiments were carried out in a flask; therefore, the temperature range was selected closed to the boiling point of *n*-butanol. The results are presented in Fig. 6.

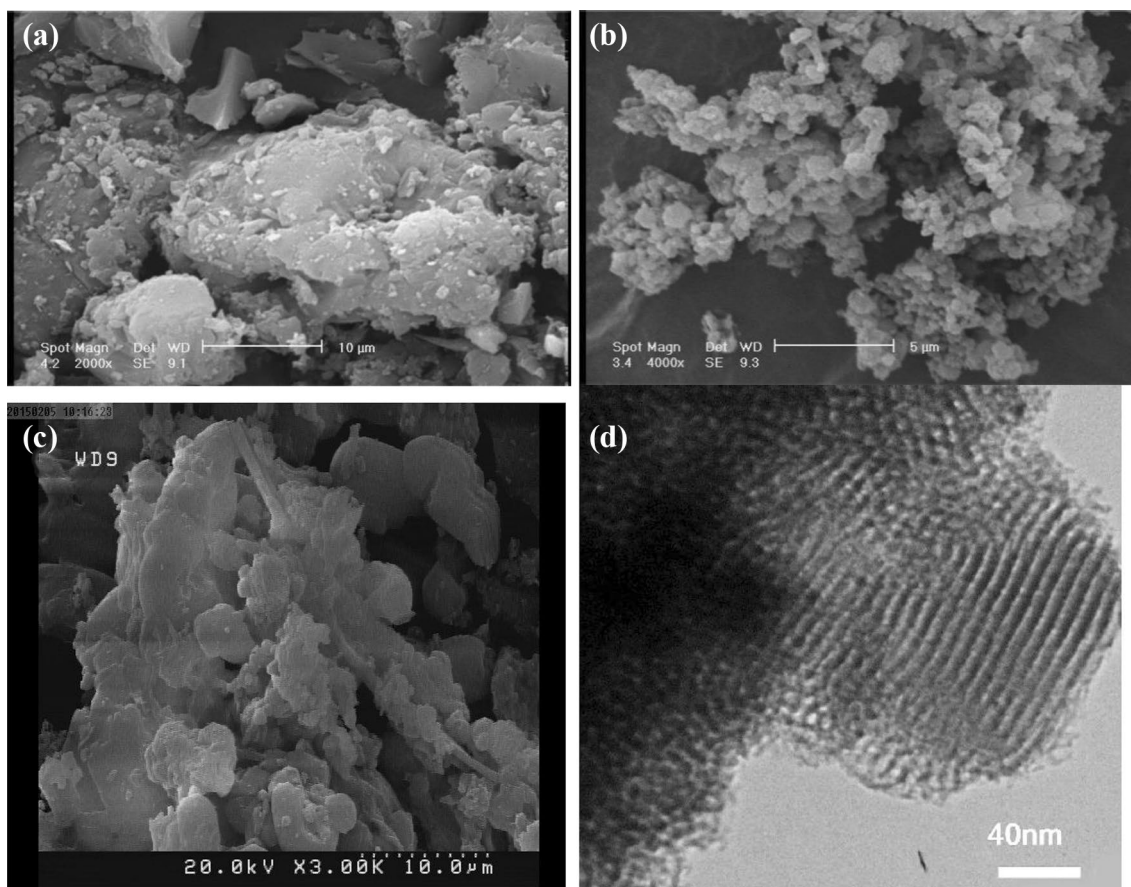
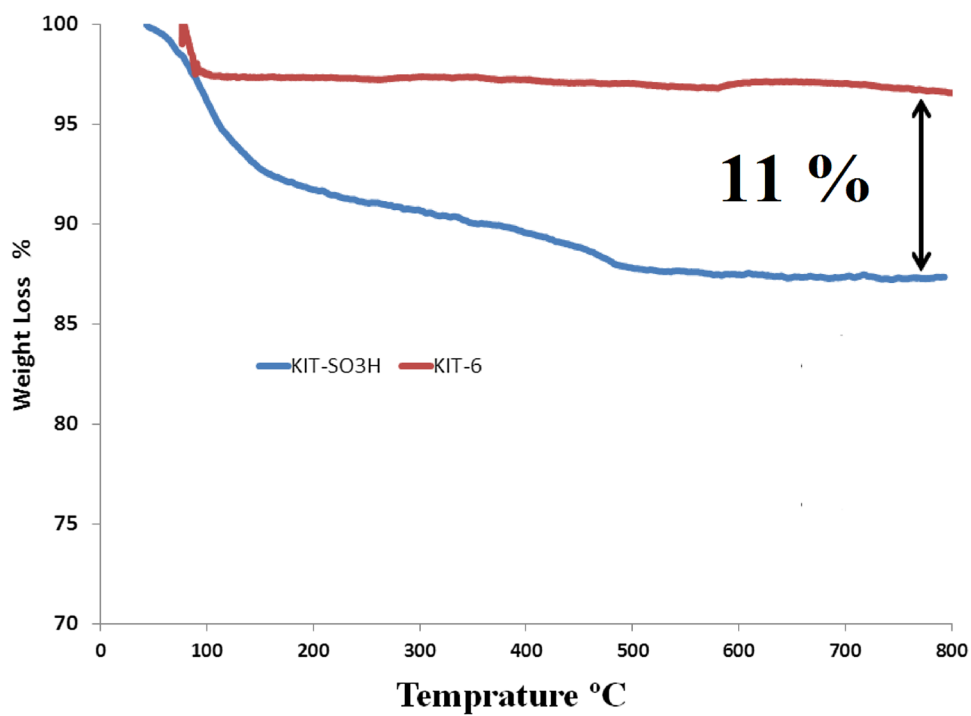


Fig. 3 SEM images of mesoporous KIT-6 (a), KIT-SO<sub>3</sub>H catalyst (b), Al-KIT-6 catalyst (c) and TEM images of KIT-6 (d)

Fig. 4 TGA curves of a KIT-6 and Al-KIT-6 samples under N<sub>2</sub>



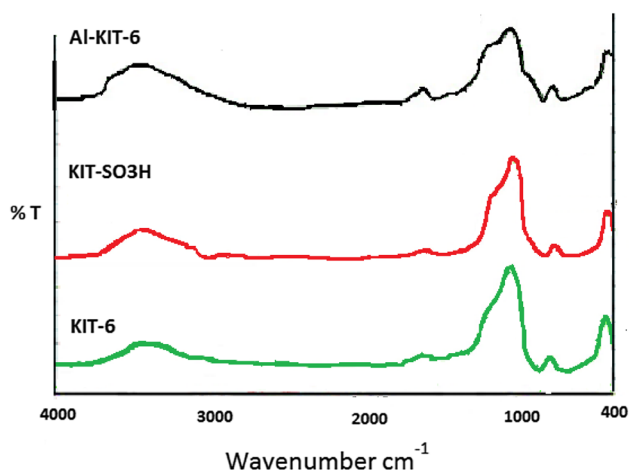


Fig. 5 FT-IR spectra of KIT-6, KIT-SO<sub>3</sub>H and Al-KIT-6 samples

The highest BL yield was reached at 90 °C. As can be seen, by increasing the temperature the ester yield increased; however, in higher temperatures the yield decreased. This may be attributed to this fact that at higher temperatures the equilibrium in the esterification reaction reversed. Therefore, 90 °C was selected as the optimum temperature in further experiments.

One of the most important parameters in the Fischer esterification reactions is the molar ratio of the alcohol to carboxylic acid. Since the esterification of LA with alcohols is a reversible reaction, by minimizing the backward reaction high conversion could be achieved. In this reaction, water is produced and due to its boiling point which is near the *n*-butanol and could not be removed during the reaction, the higher molar ratio of the alcohol should be used. However, in higher molar ratios, the molecules occupy the active sites and reduce catalytic activity. Figure 6 shows the effect of molar ratio of LA to *n*-butanol varied from 1:2 to 1:20 at 90 °C and using 10 mg KIT-SO<sub>3</sub>H catalyst and reaction time of 6 h. It is evident that with the increase in the molar ratio of LA to alcohol from 1:2 to 1:14, the ester yield increased from 11 to 59% suggesting the optimum LA-to-alcohol molar ratio is 1:14. Further increase in molar ratio to 1:20 decreased the ester yield. In all cases, the *n*-butyl levulinate selectivity was near 100%.

The study was further extended to investigation of the effect of reaction time on the esterification reaction. Figure 7 illustrates the effect of reaction time from 2 to 10 h for esterification at 90 °C and LA-to-alcohol ratio 1:14 and application of 10 mg catalyst dosage. The conversion was observed to be significantly increased up to a reaction time of 8 h from 18 to 69%. The conversion was found to

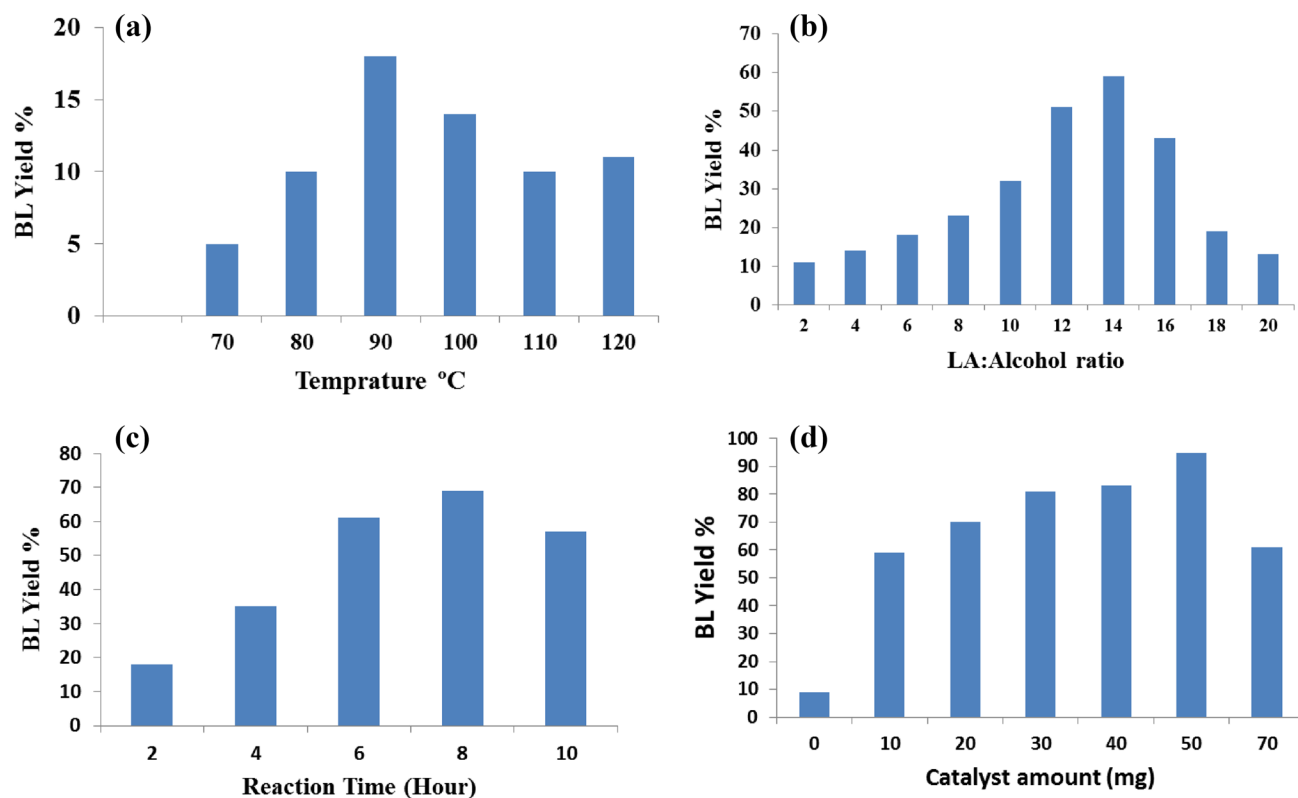


Fig. 6 Conversion of LA to BL under different conditions. Reaction condition for each case is given in the main text

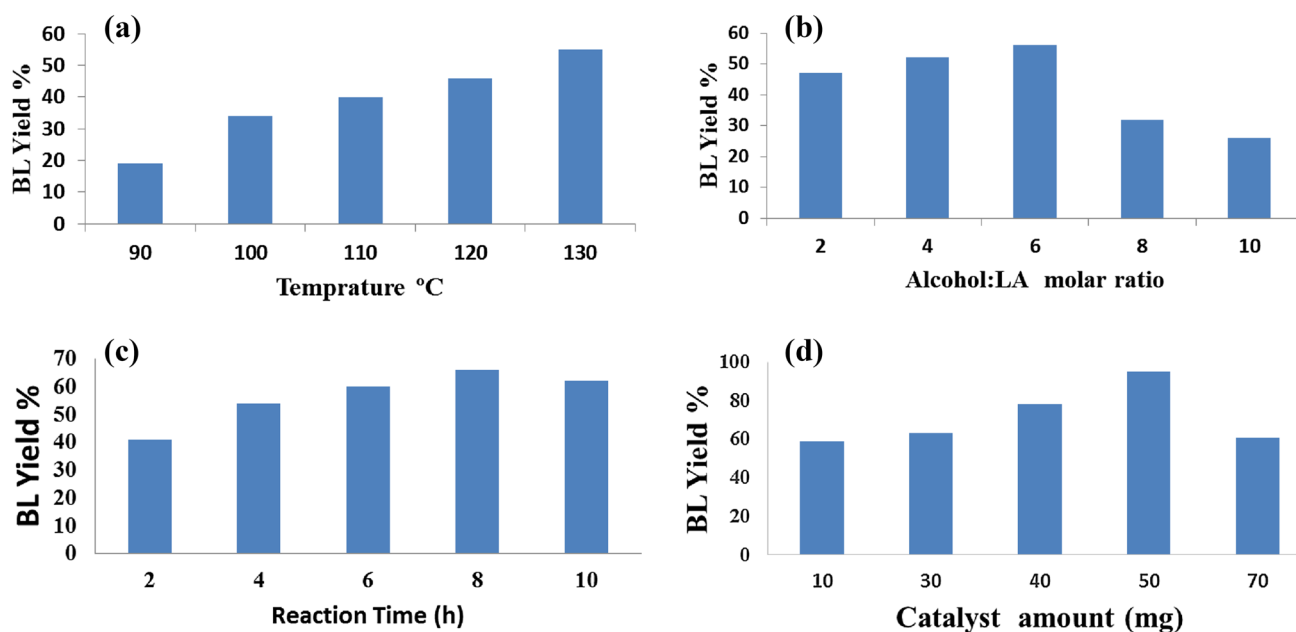


Fig. 7 Conversion of LA to BL under different conditions using Al-KIT-6 catalyst. Reaction condition for each case is given in the main text

be slightly decreased beyond 8 h probably due to reversing the equilibrium backward in prolong time. Thus, the optimum reaction time was found to be 8 h.

The effect of catalyst loading amount on the conversion of LA to BL with reaction time of 8 h, molar ratio of acid to alcohol at 1:14 and reaction temperature of 90 °C is presented in Fig. 7. A closer look at the results reveals with the increase in the catalyst amount from 10 to 50 mg, the BL yield increased from 59 to 95%. Further increase in catalyst amount decreased the product yield to 61%. Therefore, the optimum catalyst amount in this reaction was selected as 50 mg KIT-SO<sub>3</sub>H. For the demonstration of catalytic activity of KIT-SO<sub>3</sub>H, a reaction under optimum condition (90 °C temperature, 8 h, alcohol to LA 1:14) without catalyst was performed, and according to GC analysis, 9% BL was observed. The levulinic acid esterification with alcohols occurs even in the absence of catalyst due to auto-catalyzed reaction by itself.

In the next stage and in comparison with the catalytic activity of Al-KIT-6 with KIT-SO<sub>3</sub>H catalyst, the esterification reaction LA with *n*-butanol was carried out and the results are presented in Fig. 7.

The effect of temperature in the range 90–130 °C on the esterification reaction of LA with *n*-butanol was examined on Al-KIT-6 catalyst, and the results are presented in Fig. 7. The results indicated that the BL yield was improved with the increase in the temperature. When the temperature rose to 130 °C, the BL yield increased to 55%. Thus, the selected temperature for further studies was 130 °C.

In the next step, the effect of *n*-butanol-to-LA molar ratio was examined by using 10 mg Al-KIT-6 catalyst at 130 °C for 4 h reaction times was examined. The *n*-butanol-to-LA molar ratio varied from 2 to 10, and the results are depicted in Fig. 7. A closer look at the results indicates with the increase in the alcohol-to-LA ratio from 2 to 6, the yield increased from 47 to 56%. However, further increase in molar ratio to 1:10 decreases BL yield probably because of mass transfer limitation caused by dilution. So in this part, molar ratio of LA to ethanol 1:6 was chosen as the optimum ratio.

To evaluate the catalytic activity of Al-KIT-6 catalyst, its performance was examined at different reaction times under constant other reaction conditions including temperature 130 °C, catalyst loading 10 mg and *n*-butanol-to-LA ratio of 6. As shown in Fig. 7c, the maximum yield of BL (66%) reached at a reaction time of 8 h. When the reaction time was prolonged to 10 h, the yield decreased to 62%.

Subsequently, the effect of the catalyst dosage on the esterification reaction was assessed by changing the amount of Al-KIT-6 from 10 to 70 mg under optimum reaction conditions: reaction temperature 130 °C, molar ratio of 8:1 of *n*-butyl alcohol to LA and reaction time of 8 h. Generally, by providing more active sites the catalytic activity along with the increasing catalyst amount could improve. The results shown in Fig. 7d show that with the increase in catalyst amount from 10 to 50 mg, the BL yield changed from 66 to 95%. Nevertheless, when catalyst dosage is increased to 70 mg the BL yield decreased to 73%. The results are in agreement with the reported similar studies in the literature

[33]. This observation may be attributed to this fact that more availability of active sites may facilitate the revers esterification reaction. Therefore, under the optimum conditions including reaction time 8 h, temperature 130 °C, molar ratio of 8:1 of *n*-butyl alcohol to LA and catalyst amount of 50 mg, a relatively high *n*-butyl levulinate yield of 95% over Al-KIT-6 catalyst was obtained.

One of the most important benefits of heterogeneous catalysts is their ability for regeneration and recycling for successive runs. In fact, due to economic and environmental purposes the stability of a heterogeneous catalyst is critical.

After each catalytic run, the catalysts (Al-KIT-6 as well as KIT-SO<sub>3</sub>H) was recovered by centrifugation, washed by acetone and water (two times), and dried in oven for the use in the next run. Herein, the reusability of two catalysts was evaluated for six cycles (Fig. 8). For the KIT-SO<sub>3</sub>H catalyst, the catalytic activity was retained in three successive runs. However, the catalytic performance gradually decreased so that at 6th run the BL yield was 40%. Since the reactions were performed at the relatively high temperature and prolonged time, deactivation of the catalyst may be attributed to breaking down of propylsulfonic acid groups. The CHNS analysis evidenced the sulfur content decreased to 0.59%. For the Al-KIT-6 catalyst, the performance of the catalyst was observed to be stable for four runs with slight. However, the catalytic activity slightly decreased from the fifth run.

This may be attributed to deposition of products or intermediates on the surface of the catalyst.

Table 2 shows the results of comparison between activity of KIT-SO<sub>3</sub>H and Al-KIT-6 compounds and other catalysts reported in the literatures for the esterification of LA with *n*-butanol. A literature survey illustrated that the present study is more efficient than the earlier reported values. Maheria et al. [34] reported maximum BL yield was obtained as 82.2% using H-BEA zeolite as the solid acid catalyst. Dharne and Bokade used dodecatungstophosphoric acid supported on montmorillonite K10 as the heterogeneous catalyst in the esterification of LA with *n*-butanol and obtained 97% BL yield. However, the catalyst was reused only for two cycles [35].

Recently, Jiang et al. have studied esterification LA with *n*-butanol by using lipase-based biocatalyst. They reported 74.59% of ester yield after 12 h of reaction time [36]. Song and co-workers were synthesized series of heteropoly acid and ZrO<sub>2</sub> bifunctional organosilica nanotubes (PW<sub>12</sub>/ZrO<sub>2</sub>-Si(Et)Si-NTs) and studied their catalytic activity in the esterification reaction. They reported 69.4% BL yield after 1 under reflux temperature [37]. Zhou et al. prepared ammonium co-doped phosphotungstic acid and used as the catalyst in the synthesis of BL. They reported the yield of esterification reaction as 99% after 2 h reaction time without catalyst recycling [38].

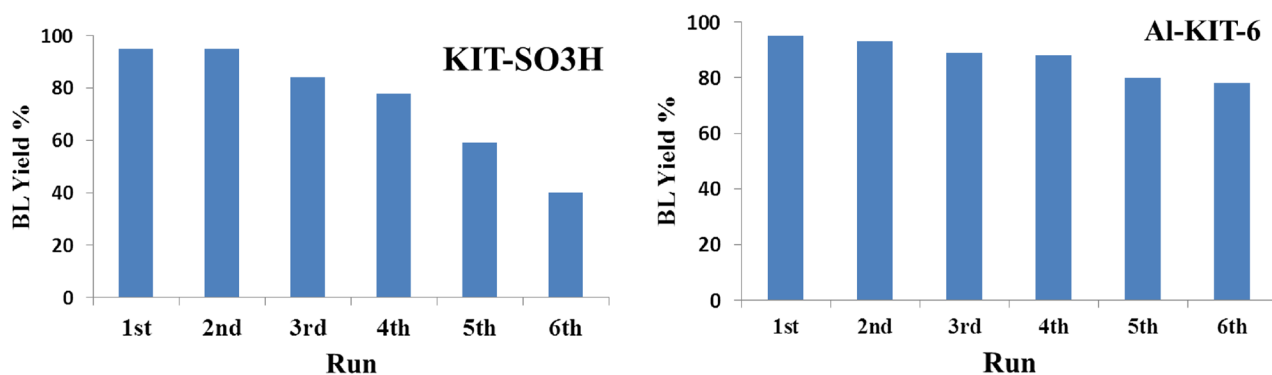


Fig. 8 Recycling of the catalysts in the esterification of LA with *n*-butanol under optimum reaction conditions

**Table 2** Comparison of the yields of *n*-butyl levulinate obtained in the present study with those reported in the literature

Entry	Catalyst	Time (h)	Temperature (°C)	Yield %	References
1	H-BEA zeolite	4	120	82.2	[34]
2	HPA/K10	4	120	97	[35]
3	Immobilized lipase	12	40	74.5	[36]
4	PW <sub>12</sub> /ZrO <sub>2</sub> -Si(Et)Si-NTs	1	120	69.6	[37]
5	(NH <sub>4</sub> ) <sub>0.5</sub> Ag <sub>0.5</sub> H <sub>2</sub> PW	2	120	99	[38]
6	KIT-SO <sub>3</sub> H	8	90	95	This work
7	Al-KIT-6	8	130	95	This work

## Conclusion

Ordered mesoporous KIT-6-PrSO<sub>3</sub>H organic–inorganic hybrid material and Al<sub>2</sub>O<sub>3</sub> grafted KIT-6 compound were successfully prepared and used as the catalyst in the esterification of LA with *n*-butanol. The successful formation of KIT-SO<sub>3</sub>H as well as Al-KIT-6 catalysts was confirmed by XRD, nitrogen adsorption/desorption and elemental analysis techniques. While optimum reaction conditions for the esterification of LA using KIT-SO<sub>3</sub>H catalyst were temperature 90 °C, alcohol-to-LA molar ratio 14, reaction time 8 h and catalyst dosage 50 mg, for the Al-KIT-6 the optimum conditions found to be temperature 130 °C, alcohol-to-LA molar ratio 6, reaction time 8 h and catalyst dosage 50 mg. The stability and reusability of catalysts were evaluated, and it was found that Al-KIT-6 showed better stability under reaction conditions. Therefore, the hybrid catalyst (KIT-SO<sub>3</sub>H) exhibits more efficient catalyst and reaction was carried out under milder conditions, while Al-KIT-6 catalyst was more stable.

**Acknowledgements** The authors are pleased to acknowledge the financial support provided by the Isfahan University of Technology (I.R. IRAN).

## References

- F.D. Pileidis, M.M. Titirici, *ChemSusChem* **9**, 1–22 (2016)
- K. Yan, C. Jarvis, J. Gu, Y. Yan, *Renew. Sustain. Energy Rev.* **51**, 986–997 (2015)
- L.M. Schmidt, L.D. Mthembu, P. Reddy, N. Deenadayalu, M. Kaltschmitt, I. Smirnova, *Ind. Crops Prod.* **99**, 172–178 (2017)
- Y. Kuwahara, W. Kaburagi, Y. Osada, T. Fujitani, H. Yamashita, *Catal. Today* **281**, 418–828 (2017)
- B.P. Pinto, A.L.L.F.C.P. Cardoso, C.J.A. Mota, *Catal. Lett.* **147**, 751–757 (2017)
- A. Phanopoulos, A.J.P. White, N.J. Long, P.W. Miller, *ACS Catal.* **5**, 2500–2512 (2015)
- G. Yana, L. Lu, Z. Beixiao, *Chin. J. Chem.* **30**, 327–332 (2012)
- M. Mascal, S. Dutta, I. Gandarias, *Angew. Chem. Int. Ed.* **53**, 1854–1857 (2014)
- F.D. Klingler, W. Ebertz, *Ullmann's Encyclopedia of Industrial Chemistry* (Wiley-VCH, Weinheim, 2000)
- F.H. Isikgor, C.R. Becer, *Polym. Chem.* **6**, 4497–4559 (2015)
- A. Harwardt, K. Kraemer, B. Rüngeler, W. Marquardt, *Chin. J. Chem. Eng.* **19**, 371–379 (2011)
- A. Démolis, N. Essayem, F. Rataboul, *ACS Sustain. Chem. Eng.* **2**, 1338–1352 (2014)
- G.A. Burdock, *Fenaroli's Handbook of Flavor Ingredients*, 6th edn. (CRC Press, Boca Raton, 2010)
- H.J. Bart, J. Reidetschlager, K. Schatka, A. Lehmann, *Ind. Eng. Chem. Res.* **33**, 21–25 (1994)
- Y. Gu, F. Jérôme, *Chem. Soc. Rev.* **42**, 9550–9570 (2013)
- E. Christensen, A. Williams, S. Paul, S. Burton, R.L. McCormick, *Energy Fuels* **25**, 5422–5428 (2011)
- Z. Mohammadbagheri, A.N. Chermahini, *J. Ind. Eng. Chem.* **62**, 401–408 (2018)
- A.N. Chermahini, M. Nazeri, *Fuel Process. Technol.* **167**, 442–450 (2017)
- Z. Mohammadbagheri, A.N. Chermahini, *Chem. Eng. J.* **361**, 450–460 (2019)
- Z. Babaei, A.N. Chermahini, M. Dinari, *Chem. Eng. J.* **352**, 45–52 (2019)
- I. Delidovich, K. Leonhard, R. Palkovits, *Energy Environ. Sci.* **7**, 2803–2830 (2014)
- H. Li, L. Peng, L. Lin, K. Chen, H. Zhang, *J. Energy Chem.* **22**, 895–901 (2013)
- F.D. Pileidis, M. Tabassum, S. Coutts, M.-M. Titirici, *Chin. J. Catal.* **35**, 929–936 (2014)
- A. Corma, H. García, *Chem. Rev.* **103**, 4307–4365 (2003)
- W. Ciptonugroho, M.G. Al-Shaal, J.B. Mensah, R. Palkovits, *J. Catal.* **340**, 17–29 (2016)
- K.Y. Nandiwale, V.V. Bokade, *Chem. Eng. Technol.* **38**, 246–252 (2015)
- M.A. Tejero, E. Ramírez, C. Fité, J. Tejero, F. Cunill, *Appl. Catal. A Gen.* **517**, 56–66 (2016)
- X. Zhou, Z.X. Li, C. Zhang, X.P. Gao, Y.Z. Dai, G.Y. Wang, *J. Mol. Catal. A Chem.* **417**, 71–75 (2016)
- F.G. Cirujano, A. Corma, F.X.L. Xamena, *Chem. Eng. Sci.* **124**, 52–60 (2015)
- A.N. Chermahini, N. Andisheh, A. Teimouri, *J. Iran. Chem. Soc.* **15**, 831–838 (2018)
- A. Prabhu, L. Kumaresan, M. Palanichamy, V. Murugesan, *Appl. Catal. A Gen.* **360**, 59–65 (2009)
- F. Kleitz, S.H. Choi, R. Ryoo, *Chem. Commun.* **9**, 2136–2137 (2003)
- B.R. Jermy, A. Pandurangan, *J. Mol. Catal. A Chem.* **237**, 146–154 (2005)
- K.C. Maheria, J. Kozinski, A. Dalai, *Catal. Lett.* **143**, 1220–1225 (2013)
- S. Dharna, V.V. Bokade, *J. Nat. Gas Chem.* **20**, 18–24 (2011)
- L. Zhou, Y. He, L. Maa, Y. Jiang, Z. Huang, L. Yin, J. Gao, *Biore-sour. Technol.* **247**, 568–575 (2018)
- D. Song, S. An, Y. Sun, Y. Guo, *J. Catal.* **333**, 184–199 (2016)
- X. Zhou, Z.X. Li, C. Zhanga, X.P. Gao, Y.Z. Dai, G.Y. Wang, *J. Mol. Catal. A Chem.* **417**, 71–75 (2016)